Design and validation of an articulated solar panel for CubeSats

Patrick Höhn
Dwarf Planet Project
Adalbertsteinweg 218, 52066 Aachen, Germany
hoehnp@dwarfplanetproject.de.vu

ABSTRACT

CubeSats are recently adopted for increasingly advanced mission profiles, e.g. as base for tests of solar sails or formation flight. This also leads to higher power demands on-board of the satellite. Currently most CubeSats are equipped with solar cells on their surface. Some satellites also employ additional deployable solar panels with a fixed end angle to meet the increasing power demands. Further improvements are attempted in the current work by including actuators which allow the movement of the deployable solar panel in one degree of freedom.

The proposed design is based on a small stepper motor which is incorporated with a planetary gear-head. The selected material for most of the components iss aluminum to minimize the mass of the system. After the completion of the design, the system was validated by vibrational and thermal computational analyses. A prototype of the final design was manufactured for tests and validation of the computational simulations. Vibrational tests were performed at the Space Dynamics Lab of Utah State University for the vibrational loads during a simulated launch. A comparison of the frequency of the first vibration mode showed a reasonable agreement between simulations and validation test.

INTRODUCTION

CubeSats have become a low-cost and fast alternative to bigger satellites in the recent years. Many components were successfully miniaturized. The stabilization types changed from simple spin stabilization and passive stabilization using permanent magnets to fully three-axis stabilized spacecrafts. Some recent missions also validated propulsion systems for CubeSats. Despite this tremendous progress, two problems remain unsolved due to the small surface area of CubeSats with fixed body panels: energy generation and heat dissipation. One possible solution is to enlarge the available surface area by the usage of deployable structures.

The developed design is based on a generic CubeSat mission and an orbit with an altitude of 400 kilometers and an inclination of 40 degrees during the year 2011. The satellite is assumed to be three-axis stabilized. In order to validate the survivability of the mechanism for launch vibration analyses and tests have to be performed. Damages of the mechanism and the satellite panels are usually prevented by locking them in a stored position and releasing them after reaching the final orbital position.

In general, mechanisms on board of CubeSats are limited to small dimensions and masses by the CubeSat launch containers. Further details can be found in the CubeSat specification.[1] Working in an environment with no possibility of later corrections or modifications requires a high functional reliability and repeatability. The two major impacts on the satellite are the compatibility of the thermal heat expansion ratios and the large occurring temperature changes. These result in thermally induced stresses which might cause cracks in components or delamination of glued components like solar cells. This can be prevented by the use of materials with a similar coefficients of thermal expansion.

Beside the constraints discussed earlier, solar cells degrade during their lifetime. Therefore it is common practice to design solar panels with a higher energy output at the beginning of the mission to meet the requirements at the end of the mission.

Another critical issue is the electric connection of the solar panel to the satellite bus. The most common solutions in this field are cables and slip ring devices.

This report focuses on the use of deployed or articulated solar panels to generate the required energy during the whole mission. Hence, it presents the results of an evaluation for the design of the subsystems of a deployable or articulated solar panel for CubeSats. Afterwards, the environmental challenges during launch and orbiting phase are briefly introduced. This leads to the problem statement which states the requirements of the proposed articulated solar panel. Thereafter, the conceptual proposed design and a more detailed specification are presented. The paper closes with an computational and experimental validation of the proposed design and final conclusions.

SUBSYSTEMS

The suggested system was analyzed with respect to four different groups, release mechanisms, mechanisms for articulation, control mechanisms and types of solar cells. An extensive study of many solution options can be found in [2]. Here, only the selected options for the different subsystems are summarized.

Release mechanisms

During the launch of any spacecraft, external larger structures are stowed for space reasons in the positions with the minimum volume. In order to avoid damages to the spacecraft the deployable parts are secured by additional measures. One measure can be fixing the movable components by ropes or wires.

The selected mechanism is called heat wire. It was selected for its simplicity, long space heritage and high reliability. One example for the application on a CubeSat is the CUTE-1 mission of Tokyo Institute of Technology for securing the attached antennas in the stowed location. [3]

The mechanism is based on the fact that the tensile strength of a wire decreases when heated up until it reaches its melting point. In this case the heat is delivered by a small heat winding which is powered at the desired time of release. Depending on the geometry of the wire and the power of the heat winding, the wire might be destroyed by a lowered ultimate strength or ultimately by melting the wire.

Articulation mechanisms

Articulation mechanisms are used to adjust the orientation of the solar panels with respect to the main body of the satellite to achieve the optimal sun-incident angle.

Among the evaluated options stepper motors were selected, as they offer a high flexibility and precision for the articulation process. Furthermore, stepper motors have already been used in space applications and offer a good controllability which is highly beneficial for an accurate positioning of the solar panels. Further improvements in the positioning accuracy and torque can be achieved by the use of a gearing. The most space-efficient way to construct such a gearing was found to be a planetary gearing.

Control mechanisms

Electronic controllers are widely used in any field of engineering. They also have a long heritage in space applications.

As the satellite already includes an avionics system, an electronic controller could be easily implemented. Considering simple PID controllers it would be required to utilize an additional sensor or estimator for determining the sun-incident angle. However, as the sensor requires additional space and mass another alternative could be the application of an extremum seeking controller.

Types of Solar cells

Solar cells are the most used energy source for Earth orbiting satellites since the beginning of the space age. Since then, beginning from rigid silicon solar cells more advanced technologies like thin film solar cells were developed. In order to increase the efficiency further other materials, like Gallium-Arsenide, and more layers for different spectral bands were introduced.

The complete power system of a spacecraft consists of the energy source, – in this section solar cells – batteries, a power control system and the wiring. In order to generate the required electric currents and voltages solar cells are in series and in parallel. Voltage requirements are met by series connections, while current requirements make use of parallel circuits.

Solar cells experience degradation during their lifetime. Cover-glass that protects the active material of the cells changes its translucency due to solar UV radiation. [4] Another notable degradation source is particle radiation.

The selected type of solar cells are triple-junction solar cells. Unlike more traditional solar cells which only use one n-p junction, this type uses three material pairings to cover a larger part of the spectrum of the electromagnetic radiation. Solar cells in 2010 provided a conversation efficiency of 28.3 percent and experience a 15 percent degradation by 1 MeV in 33 years. [5]

SPACE AND LAUNCH ENVIRONMENT

Spacecrafts need to be designed to survive both the launch and the orbit environment. The first one is mostly characterized by the vibrations which place high dynamic demands on the satellite structure. Similarly, the second one is characterized by the temperature changes during one orbit. As both environments are crucial for a successful mission any design needs to be validated thoroughly to survive both.

Vibration testing

Vibrations during launch can cause severe damages of satellites sent to space. These might be caused by the loosening of parts or impacts. Therefore it is important to perform vibrational analyses and testing during the design process of any component for launch

qualification. Such tests commonly involve sine survey, random vibration and shock tests. The first one is used to investigate the modes of the oscillation for the components. Using the results requirements demanding a minimum natural frequency can be verified. Random vibration tests evaluate the influence of random oscillations during launch. The last ones are important for the understanding of the vibrations during separation maneuvers.

Computational simulations are usually based on finite element models. The sine survey is commonly named as modal analysis and also the first step for a random vibration analysis. In the second step the actual analysis is performed resulting in displacements and stresses. Random vibration simulations use spectral densities (see results section) as input for the excitation of the assembly. These can be retrieved for the specific launch vehicle. CubeSat missions use a generic acceleration spectral density which should represent all major launch vehicles. [6]

Experimental tests can be performed by the utilization of shaker tables, loud speakers or hammers as excitation sources. This article will focus on the use of shaker tables.

Thermal Issues

Space systems undergo large temperature variations of up to 200 K during an orbit. These cause thermally induced stresses between attached parts and can lead to fatigue of the material. In order to minimize this effect materials with a similar coefficient of thermal expansion should be used in any possible situation. Another possibility to reach this goal partially is the utilization of larger tolerances that allow the expansion to occur. Thus the resulting stress level is also lower compared to the restricted case.

PROBLEM STATEMENT

The generated electric energy on orbit average can be increased by at minimum P_0 =12Wh at AM0 by the use of articulated solar panels within the constraints mentioned below:

- Output voltage between 16 and 20 volts

- Embedded torque coil including interface

- Temperature sensor at back side of panel

- Possibility to print antenna circuit on or with in the array substrate without degradation of array performance

- Electrical interface for antenna, torque coil, power and temperature sensor

- Size:

    o 10x30x0.6 cm (placed completely outside of spacecraft) for deployed solar array

    o 10x30x1.6 cm for articulating solar array

- Mass: 182.5 gram

- Compliance to the launch loads specified in NASA GEVS

- Compatibility with on orbit temperatures

- Compatibility of thermal expansion / contracting of all used materials

CONCEPTUAL DESIGN

Based on the selected submechanisms the final design for the panel is described below. The middle part consists of a brush-less electric motor and a corresponding planet gear head, i. e. the ADM 0620 and 06/01 16:1 from Micromo Inc. These provide a precision of 0.6 degrees in half step mode. They are attached by three set screws to the middle connector which in terms is screwed to the satellite body. For articulation the right active part of the hinge is attached by two the set screws to the outgoing shaft of the gear box. The outer parts are completely passive. They consist of the left and right connector, the hinges and shafts which attach the different parts by the utilization of retaining rings. A proper position of the hinge with respect to the shaft is achieved by connecting both with set screws similar to the hinge at the opposite side.

In order to meet the requirements for the mechanical envelope, the whole mechanism is mounted at the satellite partially inside of it, i. e. the side face of the satellite is placed above face of the joints. This is depicted in Figure 1.
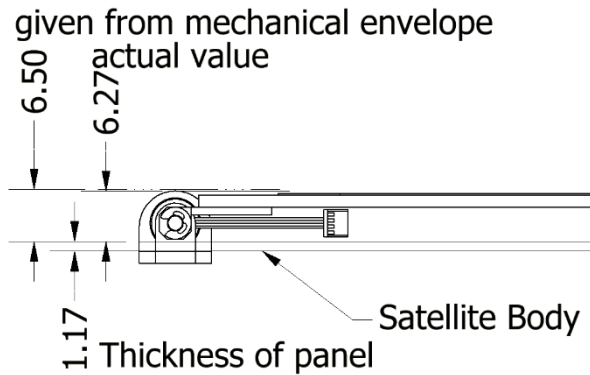
Figure 1: Compliance to mechanical envelope

Figure 2 depicts the dummy solar panel attached to the mechanism shown in Figure 3. The panel is manufactured as a PCB in order to simplify the harnessing and to reduce weight. It is designed with one internal copper layer for the harnessing and the embedding of torque coils and/or antennas with contacts at the appropriate side of the board.

Figure 2: complete design including the attached dummy solar panel

All solar cells are connected in series. Using the cables soldered to the connector pins at the right, the solar panel is connected to a socket at the top of the satellite. For the use of the proposed socket and plug (DF13-10S-1.25C and DF13-10P-1.25DS from 7) it might be necessary to place the socket partially inside of the satellite. One temperature sensor, one home switch, one heat winding and three rubber pads, one in a central position and two at the far corners, are attached to the back side. The two later mentioned are used to decrease the response of the panel to launch induced vibrations. Loosening of screws during launch is prevented by the securing them with epoxy.

Figure 3: Overview of complete mechanism without solar panel

On orbit, the wire pressing the pads to the satellite body will be cut by the heat winding. Afterwards the panel can be articulated by the motor and its control electronics, as claimed in the thesis statement. The home switch is used to reset the position pointer to a specific reference position.

DETAILED SPECIFICATION

Before starting with the design of the actuation devices some of the requirements, in particular regarding temperature and power, need further refinement. This will result in some key parameters, like a specified temperature range or the required area of solar cells. Afterwards, the motor is derived from the given parameters.

Worst case temperatures

The influence of the dissipated heat of the satellite on the temperature of the deployed solar panels can be neglected. Thus, the only contribution is the incident IR radiation. The used parameters are summarized in Table 1.

Table 1: Parameters used for the calculations in this section

Symbol	Value	Description
h	400 km	Orbital Altitude
G_S	1367 W/m^2	Solar constant, average value
α_S	0.92	Absorptivity of Solar cells, value from 8
ε_S	0.85	Emissivity of Solar cells, value from 8
ε_{BS}	0.84	Emissivity of the back side of the solar panels (assumed black paint 3M Black Velvet, see 9)
i	40°	Inclination of orbit
a	0.57	Earth's albedo (see 10)
R_E	6378 km	Earth's radius
q_{EIR}	257 W/m^2	Earth's emitted black body IR radiation (see 10)

σ	5.67 10⁻⁸ W/(m² K)	Stefan-Boltzmann constant
q_{SC}	227 W/m²	Power converted to electricity (see next section)

As the solar panels are deployed away from the satellite, the heat influx from the satellite body can be neglected. The remaining incoming heat consists of direct solar flux, albedo and Earth IR. The first can be expressed by the following term:

$$q_{Solar} = G_S \cdot \alpha_S - q_{SC} = 1031 \frac{W}{m^2}$$

Contributions from the albedo are calculated by:

$$q_{albedo} = G_S \cdot \alpha_S \cdot a \cdot K_a \cdot sin^2\rho,$$

where:

sin(ρ)   angular size of Earth

K_a factor for correction of reflection from the spherical Earth is.

Using the following formula the necessary angular size can be determined:

$$\rho = arcsin\left(\frac{R_E}{r}\right) = 1.226$$

By using this value the correction factor is:

$$K_a = 0.664 + 0.521 \cdot \rho - 0.203 \cdot \rho^2$$
$$= 0.9976 \approx 1$$

Now the heat flux from albedo can be calculated:

$$q_{albedo} = 633.43 \frac{W}{m^2}$$

The remaining heat fraction is the Earth emitted infrared radiation:

$$q_{IR} = q_{EIR} \cdot \varepsilon_S \cdot sin^2\rho = 193.49 \frac{W}{m^2}$$

Therefore the incoming heat flux sums to:

$$q_{in} = q_{Solar} + q_{albedo} + q_{IR}$$
$$= (1031 + 633 + 193)\frac{W}{m^2}$$
$$= 1857 \frac{W}{m^2}$$

The emitted heat energy from the spacecraft is under the assumption of a sun light incident side fully covered by solar cells:

$$q_{out} = (\varepsilon_S + \varepsilon_{BS}) \cdot \sigma \cdot T^4$$

where T represents temperature of the corresponding surface.

Rearranging the formula leads under the assumption of equilibrium conditions to the temperature of the satellite:

$$T = \sqrt[4]{\frac{q_{in}}{(\varepsilon_S + \varepsilon_{BS}) \cdot \sigma}}$$

Putting in all known values delivers the surface temperature for the hot case:

$$T = \sqrt[4]{\frac{1857 \frac{W}{m^2}}{(0.85 + 0.84) \cdot 5.67 \cdot 10^{-8} \frac{W}{m^2 \cdot K^4}}} = 373K$$
$$= 100°C$$

The resulting temperature for the cold case is calculated by neglecting the solar and albedo radiation:

$$T = \sqrt[4]{\frac{193 \frac{W}{m^2}}{(0.85 + 0.84) \cdot 5.67 \cdot 10^{-8} \frac{W}{m^2 \cdot K^4}}} = 212K$$
$$= -61°C$$

Remembering the worst-case assumptions, the resulting temperature should be in reality a little bit smaller.

Estimated required solar array area

An important parameter for the evaluation of different solar array techniques is the solar array area required for given power requirement. This will be determined in this section. The required orbit average power of 12 Wh (see section Problem Statement) gives the power needed from the solar panel. Some of the parameters used in this section are summarized below:

Table 2: Parameters used for the calculations in this section

Symbol	Value	Description
h	400 km	Orbital Altitude
i	40°	Inclination of orbit
G	6.67·10⁻¹¹ (N·m²)/ kg²	Universal gravitational constant
R_E	6378 km	Earth's radius
η	28.3 %	Efficiency of solar cells (see 8)
M_E	5.974 10²⁴ kg	Earth's mass
P_0	12 Wh	Average orbit power required from solar panel

Under the assumption of an altitude of 400 kilometers with an inclination of 40 degrees the maximum shadowing orbit fraction can be determined by:

$$\frac{\varphi}{2 \cdot \pi} = \frac{1}{\pi} \cdot arcsin\left(\frac{R_E}{R_E + h}\right) = 39\%$$

With the orbital period determined by:

$$T = \sqrt{\frac{4 \cdot \pi^2 \cdot (R_E+h)^3}{G \cdot M_E}} = 5553s = 92.6min$$

This leads to an eclipse period of:

$$T_e = T \cdot \frac{\varphi}{2 \cdot \pi} = 36.1min$$

Using all know values and the time in daylight $T_d = T - T_e$, the power provided by the solar array must be at minimum:

$$P_{SA} = \frac{(P_O)}{T_d} = 12.7W$$

Ultra triple junction solar cells have an efficiency η of 28.3 percent at BOL. Using the already known values this gives the maximum deliverable power density at BOL:

$$P_0 = \eta \cdot G_S = 386\frac{W}{m^2}$$

Using an estimated worst-case Sun incident angle ϑ of 40° and inherent degradation I_d of 0.77 [7] the available power density at BOL results in:

$$P_{BOL} = P_0 \cdot I_d \cdot cos(\vartheta) = 227\frac{W}{m^2}$$

The lifetime degradation is estimated by:

$$L_d = \left(1 - \frac{degradation}{year}\right)^{satellitelife}$$

Using the degradation per year of 2.75 percent (see [11] for GaAs solar cells) and an estimated satellite lifetime of one year the degradation becomes:

$$L_d = 0.9725$$

This results in an EOL power density of:

$$P_{EOL} = P_{BOL} \cdot L_d = 220.8\frac{W}{m^2}$$

Lastly, this gives the required solar array area of:

$$A_{SA} = \frac{P_{SA}}{P_{EOL}} = \frac{12.7W}{220.8\frac{W}{m^2}} = 0.058m^2$$

Improvements by articulated solar panels

The calculation in the previous section assumed a worst case Sun-incident angle of 40 percent. In order to decrease the determined solar array area, this section performs an analysis of the influence of the Sun-incident angle on the power generated. This is done by the use of a program from the Space Dynamics Lab of the Utah State University.
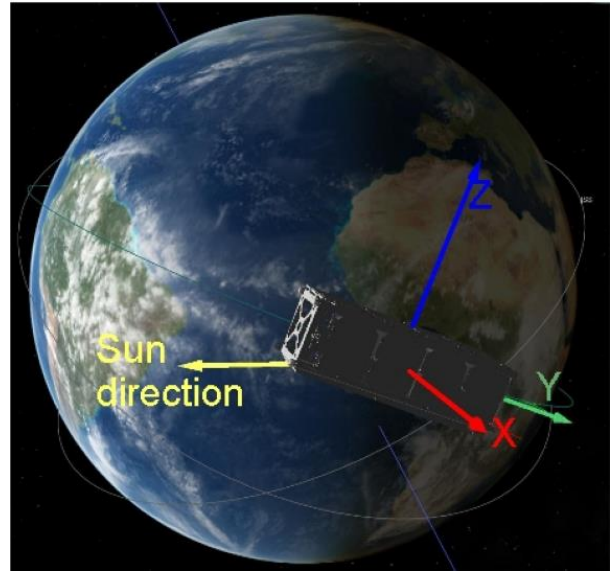

Figure 4: Attitude of satellite during Simulation (generated by Celestia)

Figure 4 shows the satellite in its orbit. One of the simulations is presented in this thesis, covering the improvements for a time step of 15 minutes throughout a complete year for body-fixed panels and panels adjusted in one and two degrees of freedom.

In the body-fixed configuration the additional panel is mounted in parallel to the +x panel. This gives an average power density of $286\frac{W}{m^2}$ during one year. By rotation about the y – axis or x – axis this value can be improved up to $817\frac{W}{m^2}$ or $496\frac{W}{m^2}$ respectively. An additional articulation in two degrees of freedom results in a slightly higher power density of $835\frac{W}{m^2}$. Thus, it is most promising to focus on a mechanism with one adjusted degree of freedom around the y-axis.

Assembly of Solar Arrays

Solar arrays are manufactured by interconnecting solar cells. The voltage requirement is met by connecting solar

cells in series, the power or current requirement by connecting them in parallel. For generating the power and voltage mentioned in the requirements, the solar array must consists of at least 8 cells in series to produce a voltage at the point of maximum power between 16 and 20 volts. The design value is 18.8 volts.

In order to generate a power of 12.7 watts (see section Problem statement) the required current is:

$$I_{mp} = \frac{P}{V_{mp}} = 0.68A$$

Using the area of each solar cell A_{SC} of $26.62cm^2$ and the current density at the point of maximum power J_{mp} of $16.3\frac{mA}{cm^2}$, this results in the number of solar cells strings needed to be in parallel:

$$n = \frac{I_{mp}}{A_{SC} \cdot J_{mp}} = 1.6 \approx 2$$

Therefore the solar array should consist of at least 2 strings of 8 solar cells, which could be realized with two deployable solar panels.

Design of Panel

The initial design of the panel was using an aluminum substrate in connection with wires for the electrical attachments. However, due to the tight mass budget and for simplification of the harnessing the material was shifted to a PCB. As described earlier, it is still attached by screws to the hinge. Unlike for the aluminum substrate the manufacturing of threads inside plastic materials is very difficult. Therefore the threads are realized by the use of inserts.

After the conduction of computational vibration analysis, it became apparent that the resulting deflections which were in the range of 60 millimeter are unacceptable, as this would cause an impact of the solar panel at both the P-POD and the satellite. This was decreased a lot by the already mentioned rubber pads for the movement away from the satellite and the heat wire for the opposite. The resulting value is around 0.5 millimeters. A more detailed description of the analysis is presented in the next chapter.

Thermal Expansion

This section gives a brief introduction to the design for compatibility of the thermal expansion of all used materials. Two different material groups are used in the scope of this analysis, i. e. Aluminum 6061 (see [12]) and

FR-2 (see [13]) for the PCB. One example depicted is the compatibility between the PCB and one of the hinges attached to it. The midpoint distance between the two outer screws is 16 millimeter. Using the corresponding thermal expansion coefficients this delivers a mismatch of:

$$\Delta l = |(\alpha_{St} - \alpha_{FR-2}) \cdot \Delta T \cdot l| = 0.02mm$$

Even though the dimensions of the model are already pretty small, this mismatch can be neglected, as it is in the range of less than one percent. Due to inaccuracies in the matching of the two hinges the probably occurring mismatch between the two different parts of the hinges is of minor interest.

The second potentially risky mismatch appears at the attachment of the passive hinge to the shaft. In this case the resulting mismatch is:

$$\begin{aligned} \Delta l = &\left| (\alpha_{St} - \alpha_{Al6061}) \cdot \Delta T \cdot l \right. \\ &= (13 - 23.6) \cdot 10^{-6}\frac{1}{K} \cdot 161K \\ &\left. \cdot 30mm \right| = 0.05mm \end{aligned}$$

This also still within a range which can be managed by the current design.

Specification of selected electric motor

The data sheet of the motor [14] states an operational temperature range of -35 to 70 °C. As the temperatures determined in section 'Worst case temperatures' exceeds this limits, an analysis based the x panel of the satellite was performed with the same parameters as given in section 'Estimated required solar array area'. This resulted in a temperature range between 16 and 20 °C. Therefore the motor is able to survive under the conditions on orbit.

The torque provided by the motor and gear-head fits the necessary torque easily as the friction is on orbit very small due to the missing gravity which acts as a normal force in an Earth's based environment.

EVALUATION AND TESTING OF THE PROPOSED SOLUTION

The evaluation performed within this thesis, includes random vibration analysis and thermal expansion analysis. While the first one is testing the performance of the mechanism during launch, the later one analyzes the thermal induced deflection and stresses during one complete orbit. Random vibration analysis are based on a power spectrum density which is taken from [15]. This computational analysis uses educational version of the program 'Algor Simulation Professional 2011' from Autodesk Inc.

Vibrational Analysis by computer based simulations

The first analysis was performed as a classical random vibration analysis based on a previous model analysis. Figure 5 depicts the shape of the first oscillation mode which has a frequency of around 240 Hertz.
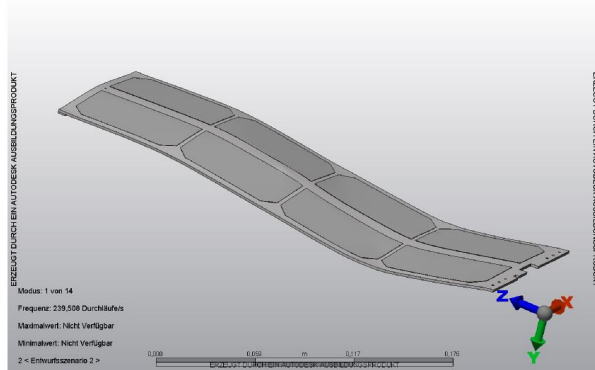

Figure 5: Shape of the first vibration mode

The panel is totally fixed its right edge and constrained in the y-direction at the pads at left end and in the center. Table shows the detected fundamental frequencies in the required range between 20 and 2000 Hertz.

Table 3: fundamental frequencies of the panel with solar cells

Mode Number	Frequency
1	239.5 Hz
2	297.3 Hz
3	353.5 Hz
4	399.5 Hz
5	522.8 Hz
6	648.8 Hz
7	848.5 Hz
8	1041.9 Hz
9	1107.4 Hz
10	1246.0 Hz
11	1304.4 Hz
12	1730.4 Hz
13	1740.1 Hz
14	1886.3 Hz

Based on the results of the modal analysis a random vibration analysis was performed for a damping rate of 1.5 percent. The results are shown in Figure 6. Despite the two fixing points at the free end, it seems like that this end undergoes the largest deflections. However, at a closer look this results from the fact that the largest deflection in this analysis appears in x direction and around 0.2 mm. The deflections in the other directions are as expected and one order of magnitude smaller than the ones in x direction.
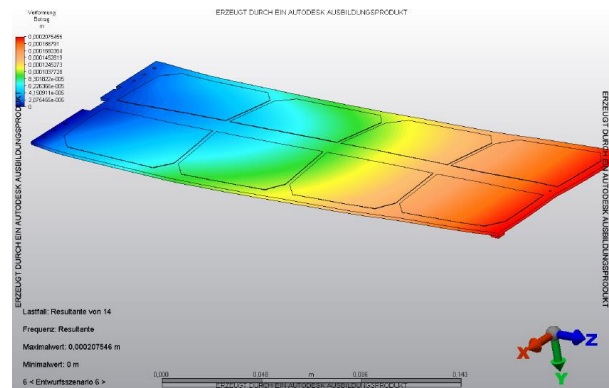

Figure 6: Absolute Deflection from classical vibrational analysis

In addition to the classical analysis as described before a time depend analysis as described in [16] was performed. The general idea behind is to convert the power spectrum density by approximation of the area below the curve in small slices to an oscillation for the specific frequency. All different oscillations are afterward superimposed at random phase angles. The resulting time series of acceleration amplitudes is then fed into a Mechanical Event Simulation which allows the simulation of a system and a time varying accelerations. The results in terms of deflection and stress are depicted in Figure 7 and Figure 8. Stress spikes in Figure 7 are calculation artifacts and disappear in a finer mesh.

All determined deflections are in a range where no damage to the components is expected. The stresses determined from the analyses, however, might exceed the limits. Therefore a redesign with another material might be necessary.
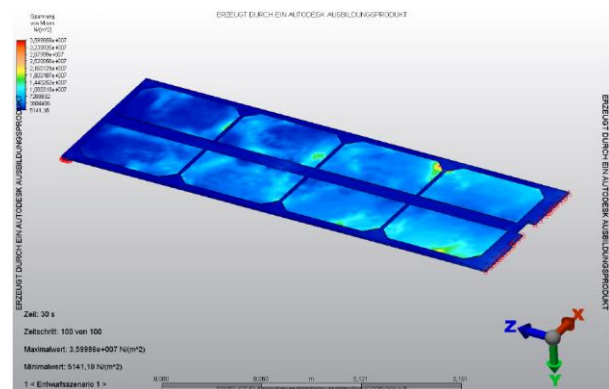

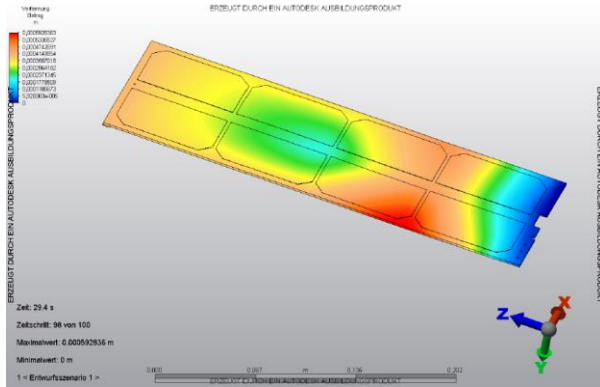**Figure 7: Resulting stress obtained by dynamic vibration study**

Figure 8: Resulting deflections obtained by dynamic vibration study

Analysis of Thermal Expansion by computer based simulations

This simulation is performed to verify that the proposed design complies with the requirement of the compatibility of the thermal expansion of all used materials. As the motor and gear-head undergo a much smaller load compared to the loads applied to the hinges it was excluded from the analysis. Temperatures change during the analysis from 0° C to 83 °C for the overall assembly. This interval is similar to the on-orbit environment. Similar to the real attachment on-board of a satellite the solar panel is fixed by four grounded screws. By the application of the above temperature changes the following figures result:
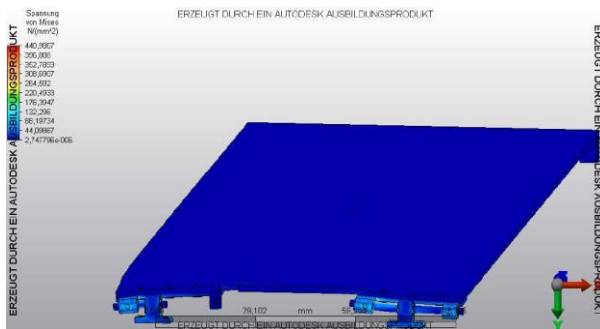

Figure 9: Resulting stresses obtained from the thermal stress analysis of the solar panel mechanism

The highest resulting highest stress of $440 \frac{N}{mm^2}$ appears within the attachments at the satellite. As this part is made from aluminum, it likely that the part will fail under the load. Thus, some components need to be changed in material to comply with the requirement of compatibility in the thermal expansion.

Evaluation by vibration test of prototype model

The computational analysis gives already a good idea of the possible problems and behavior of the panel.

However, every mathematical model has to prove its suitability and accuracy by experimental validation.

A mechanism which is supposed to work on a satellite must sustain launch and on-orbit loads. The dominating loads during the ascent phase are created by vibrations and shocks. As [15] states just random vibration loads the tests throughout this report are limited to a random vibration test in three axes.
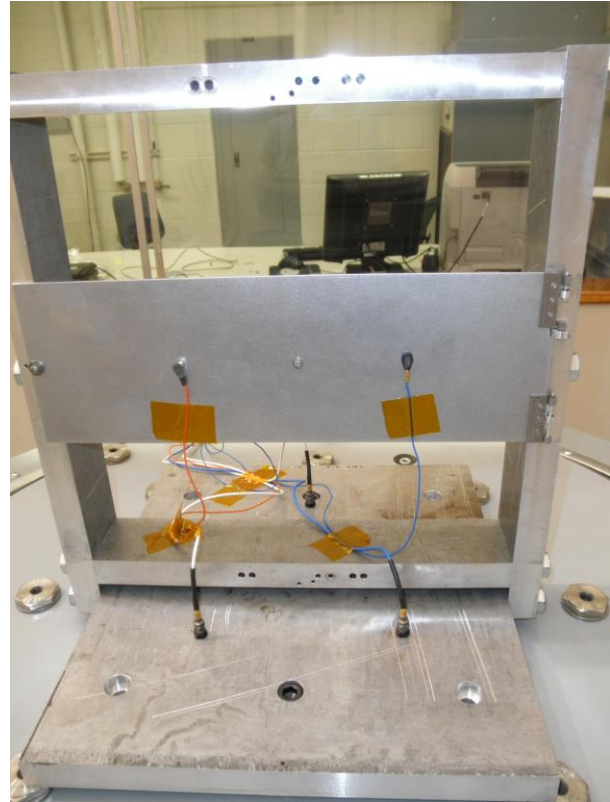

Figure 10: Sketch of the test setup of the vibrational testing

Figure 10 depicts the test setup for the vibration analysis. The block at the bottom is a placeholder for the actual attachment to the shaker table. Due to simplifications in the setup the mechanism is placed completely at the outside of the attachment. The wire going from the panel the attachment, the heat wire and the attachment is used to press the three depicted rubber pads to the attachment.

The test will be performed in as random vibration test in three axis using the power spectrum density from [15] (see Table 4) and should validate the computational analysis and the survivability of the design during launch and prove the survivability of the design.

The test is performed by following these steps:

1. Attach the accelerometers at the desired positions

2. Screw hinges to attachment

3. Move panel to the locked position.

4. Attach heat wire to panel and shaker attachment with a force in the wire of 10 N.

5. Run test for one direction.

6. Repeat steps 1 to 5 for the other two directions

Table 4: Power Spectrum Density for the random vibration test

Frequency (Hz)	Qualification ASD Level (G^2 / Hz)
20	0.026
20 – 50	+ 6 dB / octave
50 – 800	0.16
800 – 2000	- 6 dB / octave
2000	0.026
Overall	14.1 G_{rms}

Using the outlined setup above, a swept sine test and a random test were performed at the Space Dynamics Lab of Utah State University. The first determined resonance frequency was 240 Hz, which is very close to the value determined by the computational analysis.

CONCLUSION

This article presented the conclusive summary of a collection of mechanisms for actuation, guidance, damping, control and release found in literature. Other aspects like thermal and vibration issues or the design of solar panels are addressed briefly. It was shown that the power generated from a solar panel can be increased by a factor of almost 3 by the articulation around one axis. Based on the stated requirements and the literature review a new design for an articulated solar panel is suggested. It includes of a panel manufactured as a PCB. This is locked in the stowed position by a heat wire. After release it can be articulated by a small stepper motor with a precision of 0.6 degrees in half step mode.

The expected temperature range for the stepper motor lies within the operational range given in the data sheets. Thermal induced deflections and stresses exceed the limits of some of the selected materials. It is necessary to change the material of these parts from aluminum to steel. The deflections resulting from the vibrational analyses are sufficiently small to avoid damage to the solar cells, solar panel or the outside faces of the satellite.

References

1. Lee S, Hutputanasin A, Toorian A, Lan W, Munakata R. CubeSat Design Specification. 2009. Available at: http://www.cubesat.org/images/developers/cds_rev12.pdf.

2. Höhn P. Design, construction and validation of an articulated solar panel for CubeSats. 2010. Available at: http://pure.ltu.se/portal/sv/studentthesis/design-construction-and-validation-of-an-articulated-solar-panel-for-cubesats%284fb1ed72-18f9-4c74-b901-bbc9a8d1ae4b%29.html.

3. Sawada H. Tokyo Institute of Technology LSS CubeSat CUTE-I. Deploy Mech - Sol Array Paddle Deploy 2010. Available at: http://lss.mes.titech.ac.jp/ssp/cubesat/index_e.html. Accessed April 25, 2010.

4. Fortescue P, Stark J, Swinerd G. In: Spacecraft Systems Engineering. 3rd Edition. J Wiley & Sons, 2009:328–36.

5. Wertz JR, Larson WJ. In: Space Mission Analysis and Design. Third Edition, Ninth Printing. Space Technology Library. Hawthorne: Microcosm Press, 2007:414.

6. Köhler B. In: Werkstofftechnologie der Luft- und Raumfahrt. Aachen: Mainz, 2001:3–5.

7. Wertz JR, Larson WJ. In: Space Mission Analysis and Design. Third Edition, Ninth Printing. Space Technology Library. Hawthorne: Microcosm Press, 2007:433.

8. Spectrolab. 28.3% Ultra Triple Junction (UTJ) Solar Cells. 2008.

9. Wertz JR, Larson WJ. In: Space Mission Analysis and Design. Third Edition, Ninth Printing. Space Technology Library. Hawthorne: Microcosm Press, 2007:417.

10. Wertz JR, Larson WJ. In: Space Mission Analysis and Design. Third Edition, Ninth Printing. Space Technology Library. Hawthorne: Microcosm Press, 2007:412.

11. Wertz JR, Larson WJ. In: Space Mission Analysis and Design. Third Edition, Ninth Printing. Space Technology Library. Hawthorne: Microcosm Press, 2007:436.

12. Alclad Aluminum 6061-O. Available at: http://www.matweb.com/search/DataSheet.aspx?MatGUID=6c41b0bdea564d20b9fd287c03c97923&ckck=1. Accessed June 16, 2015.

13. DuPont. DuPont™ Kapton® HN.

14. Faulhaber Group. Stepper Motors - ADM 0620 PCS.

15. Brown J. Test Pod User's Guide. 2006.

16. Autodesk Whitepaper. Comparison of Experimental Shaker Table Results with Classical FEA Frequency Response Analysis vs. Mechanical Event Simulation.